Complex network analysis of wind tunnel experiments on the passive scalar dispersion in a turbulent boundary layer

Complex network analysis of wind tunnel experiments on the passive scalar dispersion in a turbulent boundary layer

Giovanni Iacobello, Luca Ridolfi, Massimo Marro, Pietro Salizzoni and Stefania Scarsoglio

Abstract In this work, experimental data of passive scalar plumes in a turbulent boundary layer are investigated. The experiments are performed in a wind tunnel where a passive scalar is injected through an L-shaped tube. Two source configurations are analysed for two different tube diameters. The passive scalar concentration is then measured at different distances from the source and wall-normal locations. By exploiting the recent advances of complex networks theory, the concentration time-series are mapped into networks, through the *visibility algorithm*. The resulting networks inherit the temporal features of the mapped time-series, revealing non-trivial information about the underlying transport process. This work represents an example of the great potentialities of the complex network approach for the analysis of turbulent transport and mixing.

1 Introduction

The understanding of the passive scalar dynamics in atmospheric boundary layer is crucial for the spatio-temporal characterization of pollutants and contaminants in dispersion processes. To this aim, a variety of strategies – mainly relying on statistical analyses – has been adopted for the investigation of concentration time-series [1].

G. Iacobello, and S. Scarsoglio
Department of Mechanical and Aerospace Engineering, Politecnico di Torino, 10129 Turin, Italy,
e-mail: giovanni.iacobello@polito.it

L. Ridolfi
Department of Environmental, Land and Infrastructure Engineering, Politecnico di Torino, 10129 Turin, Italy,

M. Marro and P. Salizzoni
Laboratoire de Mécanique des Fluides et d'Acoustique, University of Lyon, CNRS UMR 5509, Ecole Centrale de Lyon, INSA Lyon, Université Claude Bernard, 36, avenue Guy de Collongue, 69134 Ecully, France

In this work, we propose a complex network-based approach for the analysis of experimental data of passive scalar concentrations emitted by a point source in a turbulent boundary layer [1, 2]. Differently from the classical statistical tools, such as PDFs and high-order moments, complex networks are able to capture the temporal structure of the mapped time-series [3], thus revealing non-trivial features of the underlying turbulent dynamics. Following the recent advances of the network science for the analysis of turbulent flows [4, 5, 6, 7], the present work proposes a novel perspective for the analysis of experimental spatio-temporal data about the turbulent dispersion of a passive scalar.

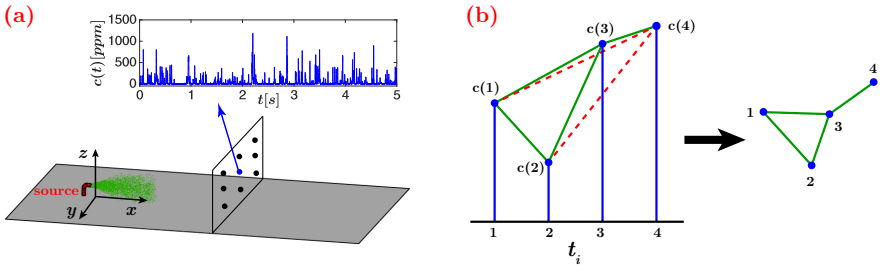

Fig. 1 (a) Sketch of the experimental setup. The source of passive scalar (ethane) is an L-shaped tube at $z_s = 75$ mm, and an example of time-series of concentration, $c(t)$, is also reported. The axis origin is put at the wall (i.e., $z = 0$) in correspondence with the source location. (b) Example of application of the visibility algorithm. A series with four temporal observations is shown as blue vertical lines (left), corresponding to the nodes of the network (right). Green solid lines represent the visibility lines between data points (see Eq. 1) and the corresponding links in the network, while red dashed lines indicate the absence of visibility (i.e., no link).

2 Experimental setup

Experimental measurements are performed in a recirculating wind tunnel (at the Laboratoire de Mécanique des Fluides et d'Acoustique at the Ecole Centrale de Lyon, France) with a working section that is 9 m long, 1 m wide and 0.7 m high. The experimental setup is the same as that adopted by *Nironi et al.* [1], even though these latter experiments were performed in another wind tunnel. By means of a grid turbulence and a row of spires placed at the beginning of the test section, a turbulent boundary layer was generated with a free-stream velocity $u_\infty = 4.94$ m/s and a thickness $\delta = 314$ mm. Wall roughness was also considered through a set of cubic elements of size $h_s/\delta = 6.37 \times 10^{-2}$. Due to its density similar to air, ethane (C_2H_6) was used as a passive tracer. The passive scalar was continuously ejected from a metallic L-shaped tube of diameter, D, located at a wall-normal height $z_s/\delta \approx 0.24$ (see Fig. 1(a) for a sketch of the setup). Two source configurations are analysed for two different diameters, $D/\delta = 9.55 \times 10^{-3}$ ($D = 3$ mm) and $D/\delta = 1.91 \times 10^{-2}$

(D = 6 mm). Concentration measurements were performed at different locations downstream of the passive scalar source (the δ value is nearly maintained at each streamwise measurement location), by means of a fast flame ionization detector [1, 2]. The sensitivity of the instrument – i.e., the slope of the (linear) relation between concentration and tension response – is ±3%, while the calibration range is (0 – 5000) ppm. The error in the first four moments of the concentration due to all the uncertainties in the experimental chain, was estimated to be up to 4.5%. The time-series of concentration were recorded for T = 180 s, with sampling frequency of 1000 Hz, resulting into $N_T = 1.8 \times 10^5$ temporal observations. In the following, the streamwise, wall-normal and spanwise coordinates are indicated as x, y, and z, respectively (see Fig. 1(a)). Specifically, all results are intended at $y = 0$, i.e. along the source-axis at different streamwise and wall-normal locations, in the range $x/\delta = 0.162 - 2.602$ and $z/\delta = 0.0955 - 0.685$, respectively.

3 Network building

The time-series of ethane concentration were investigated by exploiting a complex network technique called *visibility algorithm* [8]. According to this method, each point of the time-series corresponds to a node of the network, and a link between a pair of points $(t_i, c(t_i))$ and $(t_j, c(t_j))$ exists if the condition

$$c(t_k) < c(t_j) + \left(c(t_i) - c(t_j)\right) \frac{t_j - t_k}{t_j - t_i}, \tag{1}$$

is fulfilled, for any $t_i < t_k < t_j$. From a geometrical point of view, in a visibility-based network a link exists if the straight line connecting two points of the series lies above the other in-between data, thus resulting in a convexity criterion. Although the visibility algorithm is simple to implement, it is invariant under affine transformations (i.e., rescaling and translation of both horizontal and vertical axes). By exploiting the condition in Eq. 1, networks with N_T = 180000 nodes were built in each spatial location where concentration measurements are performed.

Among a broad number of network metrics proposed so far [9], two metrics were here explored to extract information of the temporal structure of the series under investigation [7]: the *mean link-length*, $\langle d_{1n} \rangle$ and the *transitivity*, Tr. In particular, $\langle d_{1n} \rangle$ is a measure of the occurrence of extreme events (i.e., peaks) in the time-series, with high $\langle d_{1n} \rangle$ values if peaks appear sporadically. On the other hand, the transitivity is related to the presence of small/null variations in the series (that we indicate as irregularities), between consecutive peaks. By combining the behaviour of the mean link-length and the transitivity, therefore, it is possible to infer the temporal structure of the mapped time-series in terms of peak occurrence and irregularity intensity [7].

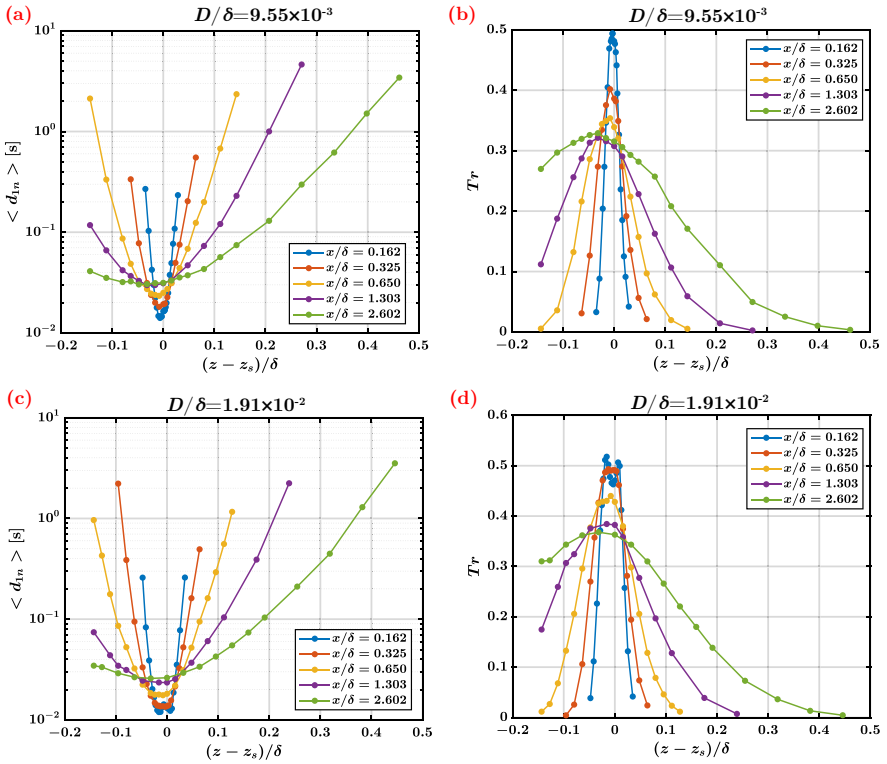

Fig. 2 Network metrics as a function of the normalized wall-normal coordinate $(z - z_s)/\delta$, for different streamwise locations, x. Mean link-length (a) and transitivity (b) when $D/\delta = 9.55\times10^{-3}$. Mean link-length (c) and transitivity (d) when $D/\delta = 1.91 \times 10^{-2}$.

4 Results

The results of the visibility network-based analysis applied to the passive scalar concentration time-series are here reported and discussed. Results of both diameter configurations are shown in Fig. 2. In particular, the mean link-length, $\langle d_{1n} \rangle$, and the transitivity, Tr, are plotted as a function of the normalized wall normal coordinate $(z - z_s)/\delta$, for increasing streamwise locations. Moreover, in order to highlight the significance of the metrics with respect to the dynamics of the passive scalar plume, in Fig. 3 we display two (normalized) time-series of concentration at two wall-normal coordinates, $(z - z_s)/\delta = 0$ (source-axis) and $(z - z_s)/\delta = 0.27$.

First, let us focus on the configuration with the smallest D/δ. As illustrated in Fig. 2(a), $\langle d_{1n} \rangle$ increases by moving away from the source-axis (i.e., $(z - z_s)/\delta = 0$), and along the streamwise direction (at fixed wall-normal coordinate). High values of the passive scalar concentration are frequently detected along the source-axis, at fixed wall-normal coordinate (e.g., see the series in Fig. 3(a)), where the relative dispersion of the plume is weak, thus low $\langle d_{1n} \rangle$ values are obtained. On the other hand, the

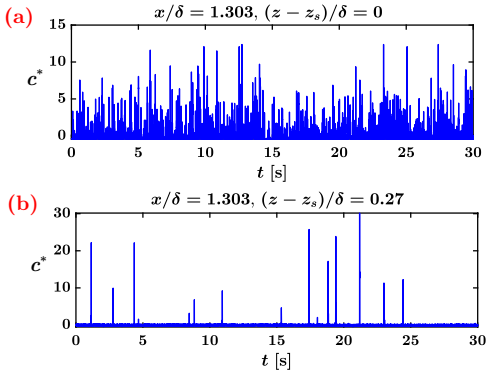

Fig. 3 First 30 seconds of the time-series of ethane concentration at two different wall-normal coordinates, for $D/\delta = 9.55 \times 10^{-3}$: (a) $(z - z_s)/\delta = 0$, namely at the centreline; (b) $z/\delta = 0.271$. For comparison purposes, the time-series are normalized as $c^*(t) = (c(t) - \mu_c)/\sigma_c$, where μ_c and σ_c are the mean and standard deviation of the local time-series $c(t)$, respectively.

mean link-length increases in the wall-normal direction, because the occurrence of concentration measurements decreases along z as a consequence of the relative dispersion of the plume (e.g., see Fig. 3(b)). Moreover, we found higher $\langle d_{1n} \rangle$ values by moving downstream along x for wall-normal coordinates close to the source-axis, because the plume weakens along the streamwise direction around $(z - z_s)/\delta = 0$. Conversely, for high $(z - z_s)/\delta$, we found lower $\langle d_{1n} \rangle$ values by moving downstream, due to the increasing spatial extension of the plume caused by the relative dispersion. These outcomes are supported by the investigation of the transitivity, Tr. We recall that low values of Tr are associated to time-series characterized by high level of irregularities, i.e. local fluctuations of low intensity (compared to the maximum excursion of the series, $c_{max} - c_{min}$). As shown Fig. 2(b), the maximum values of Tr are found along the centreline of the plume: as discussed for the mean link-length, in this region non-zero values of ethane concentration are recurrently detected (see Fig. 3(a)). On the contrary, far apart from the source-axis the temporal structure of the series of concentration is dominated by long intervals of very low intensity fluctuations (e.g., see the time interval $t \in [11, 15]$ and $t \in [24, 30]$ in the series of Fig. 3(b)), namely almost no passive scalar is measured far from the plume centreline. As a consequence, following specular trends with respect to $\langle d_{1n} \rangle$, the transitivity Tr decreases by moving away from the source-axis and along the streamwise direction.

The metrics extracted from the network built on the concentration time-series in the configuration $D/\delta = 1.91 \times 10^{-2}$ are shown in Fig. 2(c)-(d). Both the metrics highlight the same overall dynamics of the passive scalar plume discussed for the configuration $D/\delta = 9.55 \times 10^{-3}$. In fact, the minimum value of $\langle d_{1n} \rangle$ and the maximum value of Tr are found along the source centreline, while the two metrics increase/decrease moving away from the source-axis and along the streamwise direction, as in the case $D/\delta = 9.55 \times 10^{-3}$. It is worth noting that – for both D configurations – the results are asymmetrical with respect to the source-axis due to the presence of the wall. In fact, moving towards the wall $\langle d_{1n} \rangle$ is lower and Tr is higher than moving apart from the wall (by evaluating the metrics at the same wall-normal distance from the source-axis).

By comparing the magnitude of the mean link-length and the transitivity in the same

spatial locations, we found lower values of $\langle d_{1n} \rangle$ and higher Tr in the configuration $D/\delta = 1.91 \times 10^{-2}$ with respect to $D/\delta = 9.55 \times 10^{-3}$. This means that, at a fixed spatial location, the concentration for $D/\delta = 1.91 \times 10^{-2}$ is characterized by more frequent non-zero measurements, namely a higher turbulent fluctuating activity is detected. This is due to the fact that the release emitted by the larger source is submitted to a reduced spatial range of velocity fluctuations that are able to displace the scalar plume as a whole (a phenomenon usually referred to as meandering [10]), therefore inducing intermittency in the concentration signals (measured at fixed locations).

Concluding remarks

The analysis of the networks based on concentration time-series reveals that network metrics are able to highlight different spatial regions of a turbulent passive scalar plume. Specifically, the temporal structure of the mapped time-series at different spatial locations is also captured by the two metrics investigated. As a consequence, the visibility-based networks inherit the spatio-temporal structure of the underlying turbulent dynamics. Based on the present findings, the proposed approach deserves future investigation, in particular exploring to what extent the source diameter affects the dynamics of the passive scalar plume.

References

1. Nironi, C., Salizzoni, P., Marro, M., Mejean, P., Grosjean, N., and Soulhac, L., (2015), Dispersion of a passive scalar fluctuating plume in a turbulent boundary layer. Part I: Velocity and concentration measurements, Boundary-layer meteorology, vol. 156(3), pp. 415-446.
2. Fackrell, J. E., and Robins, A. G. (1982). Concentration fluctuations and fluxes in plumes from point sources in a turbulent boundary layer. Journal of Fluid Mechanics, 117, 1-26.
3. Gao, Z. K., Small, M., and Kurths, J., (2017), Complex network analysis of time series, Europhysics Letters, vol. 116(5), pp. 50001.
4. Liu, C., Zhou, W. X., and Yuan, W. K. (2010). Statistical properties of visibility graph of energy dissipation rates in three-dimensional fully developed turbulence. Physica A: Statistical Mechanics and its Applications, 389(13), 2675-2681.
5. Charakopoulos, A. K., Karakasidis, T. E., Papanicolaou, P. N., and Liakopoulos, A. (2014). The application of complex network time series analysis in turbulent heated jets. Chaos: An Interdisciplinary Journal of Nonlinear Science, 24(2), 024408.
6. Murugesan, M., and Sujith, R. I. (2015). Combustion noise is scale-free: transition from scale-free to order at the onset of thermoacoustic instability. Journal of Fluid Mechanics, 772, 225-245.
7. Iacobello, G., Scarsoglio, S., and Ridolfi, L., (2018), Visibility graph analysis of wall turbulence time-series, Physics Letters A, vol. 382(1), pp. 1-11.
8. Lacasa, L., Luque, B., Ballesteros, F., Luque, J., and Nuno, J. C. (2008). From time series to complex networks: The visibility graph. Proceedings of the National Academy of Sciences, 105(13), 4972-4975.
9. Costa, L. D. F., Rodrigues, F. A., Travieso, G., and Villas Boas, P. R. (2007). Characterization of complex networks: A survey of measurements. Advances in physics, 56(1), 167-242.
10. Gifford Jr, F. (1959). Statistical properties of a fluctuating plume dispersion model. In Advances in geophysics (Vol. 6, pp. 117-137). Elsevier.